

# GRADIENT-BASED PROGRAM SYNTHESIS WITH NEURALLY INTERPRETED LANGUAGES

000  
001  
002  
003  
004  
005  
006  
007  
008  
009  
010  
011  
012  
013  
014  
015  
016  
017  
018  
019  
020  
021  
022  
023  
024  
025  
026  
027  
028  
029  
030  
031  
032  
033  
034  
035  
036  
037  
038  
039  
040  
041  
042  
043  
044  
045  
046  
047  
048  
049  
050  
051  
052  
053  
Anonymous authors  
Paper under double-blind review

## ABSTRACT

A central challenge in program induction has long been the trade-off between symbolic and neural approaches. Symbolic methods offer compositional generalisation and data efficiency, yet their scalability is constrained by formalisms such as domain-specific languages (DSLs), which are labor-intensive to create and may not transfer to new domains. In contrast, neural networks flexibly learn from data but fail to generalise systematically. We bridge this divide with the Neural Language Interpreter (NLI), an architecture that learns its own discrete, symbolic-like programming language end-to-end. NLI autonomously discovers a vocabulary of subsymbolic primitive operations and uses a novel differentiable neural executor to interpret variable-length sequences of these primitives. This allows NLI to represent programs that are not bound to a constant number of computation steps, enabling it to solve more complex problems than those seen during training. To make these discrete, compositional program structures amenable to gradient-based optimisation, we employ the Gumbel-Softmax relaxation, enabling the entire model to be trained end-to-end. Crucially, this same differentiability enables powerful test-time adaptation. At inference, NLI’s *program inductor* provides an initial program guess. This guess is then refined via gradient descent through the *neural executor*, enabling efficient search for the neural program that best explains the given data. We demonstrate that NLI outperforms in-context learning, test-time training, and continuous latent program networks (LPNs) on tasks that require combinatorial generalisation and rapid adaptation to unseen tasks. Our results establish a new path toward models that combine the compositionality of discrete languages with the gradient-based search and end-to-end learning of neural networks.

## 1 INTRODUCTION

A central challenge in machine learning is the trade-off between symbolic and neural representations. Symbolic approaches rely on explicit rules, which enable strong compositional generalisation (Lake & Baroni, 2018), often from only a few examples (Solar-Lezama et al., 2006; Gulwani, 2011). Yet their scalability is constrained by formalisms such as domain-specific languages, which require human effort to generate, may not transfer to other domains, and are combinatorially expensive to search. Neural approaches, by contrast, scale effectively but behave as monolithic models. The knowledge they acquire is entangled within their weights, making it difficult to reuse beyond the training distribution, even when generalisation only requires recombining concepts already learned (Baroni, 2020).

In the context of program synthesis, we make progress toward bridging this divide with a model that learns its own symbolic representation, end-to-end, directly from data. Specifically, it simultaneously learns a domain-specific neural language and a neural interpreter for such a language. Similar to traditional handcrafted symbolic representations, the learned language enables compositional generalisation. Similar to neural representations, the neural interpreter’s differentiability allows us to use gradient descent to search the language-induced space for solution programs. Recent work, such as Latent Program Networks (LPNs) (Macfarlane & Bonnet, 2024), has explored learning program representations with continuous latent spaces. However, this approach is limited in its ability to generalise by composing learned concepts, which is a key strength of symbolic representations.

Our architecture, the Neural Language Interpreter (NLI), uses an encoder-decoder model to discover discrete representations (Jang et al., 2017; Maddison et al., 2016) of programs. To learn a discrete vocabulary that can represent programs in the target domain, we train on programming-by-example (PBE) tasks. During inference, conditioned on a specification of examples, NLI’s encoder produces a sequence of discrete tokens, as its internal inferred program representation. NLI’s encoder acts as a program inductor; the token sequence forms a neural program. The decoder serves as a neural executor, interpreting the program one token at a time, mapping the test input to an output, [similar to neural executors used in conditional world models Ha & Schmidhuber \(2018\)](#). Both the encoder and decoder are designed to be fully differentiable, and so NLI can be trained end to end.

Since the neural executor consumes one token at a time, NLI is not bound to a constant number of computation steps, as in previous approaches such as LPN. The number of steps in NLI’s programs can grow with the token length of programs. This is important because it enables NLI to solve problems more challenging than those with constant-time requirements, seen during training. Moreover, since NLI’s programs can recombine learned tokens in different ways and at different lengths, we hypothesise that its language supports the combinatorial generalisation lacking in previous approaches.

In addition to the engineering hurdle of designing domain-specific languages, our work is motivated by the need to bypass the difficult combinatorial search problem inherent to program synthesis. Rather than learning external guiding functions for search (Barke et al., 2020; Odena et al., 2021; Ameen & Lelis, 2023), guidance is embedded in the language NLI learns. Because the neural executor is differentiable, we can search in the space of neural programs with gradient descent. Synthesising a neural program with NLI is thus analogous to local search in symbolic spaces (Husien & Schewe, 2016), but with the advantage of having gradient signals. Another benefit of a learned language is how the search is initialised, which can dramatically affect efficiency (Hoos & Stützle, 2004; Sadmine et al., 2024). NLI’s inductor provides an initial guess for a neural program solution at test time, and the gradient search then refines this guess to find the combination of learned primitives that solves the problem.

In this paper, we introduce the Neural Language Interpreter (NLI), a model that learns its own discrete programming language and a differentiable interpreter for executing it. By combining symbolic compositionality with neural end-to-end training and gradient-based program search, NLI addresses the limitations of both paradigms. Across sequence-based compositional benchmarks, NLI achieves strong out-of-distribution accuracy on length extrapolation, primitive extraction, and novel composition tasks, where in-context learning, test-time training, and latent program networks fail. NLI matches or exceeds the performance of neuro-symbolic baselines on DeepCoder, despite training only from input–output examples without ground truth program representations.

## 2 PROBLEM STATEMENT

We formalize our task as **program induction**, where the goal is to infer the underlying behaviour of an unknown program  $p$  from input–output examples using a model  $M$ . Given a set  $S = \{(x_i, y_i)\}_{i=1}^n$  of  $n$  input–output pairs generated by  $p$  and a new query input  $x_{n+1}$ ,  $M(S, x_{n+1})$  predicts the corresponding output  $p(x_{n+1})$ . This aligns with the programming by example (PBE) formalization, where information about program  $p$  is available only via its outputs. Training tasks are formed by sampling a latent program  $p$  from a distribution  $P_{\text{train}}$  over the space of possible programs  $\mathcal{P}$ . Program specifications are formed from  $n+1$  inputs sampled from the program-dependent conditional distribution  $\{x_i\}_{i=1}^{n+1} \sim P(X|p)$ . This distribution generates inputs relevant to the logic of program  $p$ . The first  $n$  input–output pairs form the specification  $S = \{(x_i, p(x_i))\}_{i=1}^n$ , from which the model must induce the program’s logic. The model’s objective is to minimise the prediction error between its prediction,  $\hat{y}_{n+1} = M(S, x_{n+1})$ , and the true output  $p(x_{n+1})$ , to train the model to generalise program execution to a new input, not merely fit the given pairs. The model has no access to the program’s fully observable representation  $p$  during training or test time. This is vital, as real-world tasks often involve latent functions without an observable specification. At test time, the model is evaluated on programs drawn from  $P_{\text{test}}$ , which can differ from  $P_{\text{train}}$  in order to test for compositional generalisation.

108 

### 3 DISCRETE SEQUENTIAL INFERENCE

110 Existing neural program synthesis methods fail at compositional generalisation, struggling to recom-  
 111 bine learned concepts for novel tasks. The Neural Language Interpreter (NLI) overcomes this by  
 112 learning a discrete, symbolic-like programming language end-to-end. Programs are variable-length  
 113 token sequences processed by a differentiable neural executor, enabling training on input-output  
 114 examples via Gumbel-Softmax. This facilitates efficient, gradient-based search at test time to re-  
 115 fine initial programs. NLI outperforms baselines on tasks requiring combinatorial generalisation,  
 116 successfully extrapolating program lengths and synthesising novel compositions of learned skills.  
 117

118 

### 4 TRAINING OBJECTIVE

120 We train the encoder-decoder with a variational objective inspired by the ELBO. The goal is to  
 121 reconstruct a program’s output for a query input, conditioned on a specification of other input-output  
 122 pairs from the same program.

123 Formally, the program inductor  $q_\phi$  infers a latent program representation from the specification,  
 124 which the neural interpreter  $p_\theta$  then executes to predict the output for a new query. The model is  
 125 trained end-to-end on specifications of size  $n$  using a leave-one-out loss: for each pair, NLI induces  
 126 a program from the remaining  $n - 1$  pairs ( $S_i = S \setminus \{(x_i, y_i)\}$ ) and maximises the likelihood of  
 127 predicting the held-out pair. The objective is:

$$129 \quad \mathcal{L}(\phi, \theta, \mathcal{D}) = \mathbb{E}_{S_i \sim \mathcal{D}} \left[ \frac{1}{n} \sum_{i=1}^n (\mathcal{L}_{\text{recon}}(\phi, \theta; x_i, y_i, S_i) + \lambda_{\text{reg}} \cdot \mathcal{L}_{\text{reg}}(\phi; S_i)) \right] \quad (1)$$

131 where  $\mathcal{D}$  is the distribution of specifications. This objective has two components.

133 **Reconstruction Loss ( $\mathcal{L}_{\text{recon}}$ )** This term ensures that the latent program is expressive enough to  
 134 predict the program’s output on a held-out input. It is defined as the negative log-likelihood of the  
 135 target output  $y_i$  given the input  $x_i$  and the latent program  $\tilde{z}_i$  inferred from the sub-specification  $S_i$ :

$$137 \quad \mathcal{L}_{\text{recon}}(\phi, \theta; x_i, y_i, S_i) = -\log p_\theta(y_i | x_i, \tilde{z}_i), \quad \tilde{z}_i \sim q_\phi(\cdot | S_i). \quad (2)$$

139 **Encoder Regularisation Loss ( $\mathcal{L}_{\text{reg}}$ )** This regularising loss encourages reuse of tokens in the neural  
 140 vocabulary of size  $V$ , biasing the encoder (via parameters  $\phi$ ) toward discovering a compositional  
 141 latent program space. We implement a differentiable approximation of the number of unique tokens  
 142 used anywhere in the batch. By penalising programs that use many unique vocabulary entries,  $\mathcal{L}_{\text{reg}}$   
 143 promotes generalisation: the model learns to build new programs by recombining a compact set of  
 144 discovered primitives rather than memorising arbitrary token sequences for each task. The probability  
 145 of token  $k$  being chosen at position  $i$  in sequence  $b$  is denoted  $p_{b,i,k}$ , and this loss biases the encoder  
 146 toward discovering programs as reusable compositions rather than introducing a unique token for  
 147 each new program.

$$148 \quad \mathcal{L}_{\text{reg}} = \sum_{k=1}^V \left[ 1 - \exp \left( \sum_{b=1}^B \sum_{i=1}^N \log(1 - p_{b,i,k}) \right) \right]. \quad (3)$$

152 

#### 4.1 DISCRETE PROGRAM REPRESENTATION LEARNING

154 The encoder of NLI functions as a program inductor, denoted as  $q_\phi$ , from which a latent program  
 155 representation  $\mathbf{z} = (z_1, \dots, z_T)$  is sampled, given a specification  $S_i$  containing input-output examples.  
 156 This representation,  $\mathbf{z}$ , is a sequence of continuous vectors that serves as a differentiable proxy for  
 157 a sequence of discrete tokens drawn from a learned codebook of size  $K$ . This codebook includes  
 158 a dedicated skip token, which functions as a no-op, allowing the model to effectively learn shorter  
 159 programs by ignoring certain computational steps within the fixed-length sequence  $T$ .

160 For program induction firstly a transformer, which we denote by the function  $h_\phi$ , maps each  
 161 pair  $(x_j, y_j)$  in a single specification to a sequence of contextual embeddings,  $e_j = h(x_j, y_j) =$   
 $(e_{j,1}, e_{j,2}, \dots, e_{j,T})$ . These sequences are then aggregated, across the specification, by computing

162 the element-wise arithmetic mean across all  $n - 1$  pairs,  $\bar{e}_t = \frac{1}{n-1} \sum_{j=1}^{n-1} e_{j,t}$ , to produce a single,  
 163 permutation-invariant sequence of specification embeddings,  $\bar{e} = (\bar{e}_1, \bar{e}_2, \dots, \bar{e}_T)$ . In addition to  
 164 being permutation invariant, this aggregation method also enables generalisation to specification sizes  
 165 different from those seen during training, as demonstrated in Macfarlane & Bonnet (2024).  
 166

167 To obtain a differentiable proxy for a discrete program, this sequence of continuous embeddings is  
 168 projected to the codebook space. A shared multi-layer neural network  $f$  maps each embedding  $e_t$  to  
 169 a vector of logits, parameterising a categorical distribution over the  $K$  codebook entries. We then  
 170 apply the Gumbel-Softmax relaxation to sample a "soft" one-hot vector at each position  $\tilde{\pi}_t$ :  
 171

$$l_t = f(e_t) \in \mathbb{R}^K \quad \pi(e_t, \tau_p, g_t) = \text{softmax} \left( \frac{l_t + g_t}{\tau_p} \right) \in \Delta^K$$

172 where  $g_t$  is a sample from a Gumbel distribution and  $\tau$  is the temperature. The final program  
 173 representation  $z = (z_1, \dots, z_T)$  is defined as the continuous approximation of a discrete program,  
 174 which is passed to the decoder, and is constructed by taking a weighted combination of the codebook  
 175 embeddings  $V$  using these soft vectors:  
 176

$$z_t = V^\top \pi(\bar{e}_t, \tau_p, g_t), \quad z = (z_1, \dots, z_T)$$

177 During training, the temperature  $\tau$  is steadily annealed, progressively improving the approximation  
 178 of a discrete sample from the un-normalised distribution  $l_t$ .  
 179

## 180 4.2 RECURRENT NEURAL PROGRAM EXECUTION

181 A common failure point for standard decoders is that they overfit to program lengths and structures  
 182 seen during training. We implement the neural interpreter as a recurrent application of an executor  
 183 network to achieve compositional generalisation. This executor network conditions on the program  
 184 representation  $z$  one token at a time, using a shared neural executor  $d_\theta$  to iteratively update an  
 185 intermediate program state  $s_t$ . This sequential execution naturally handles novel combinations of  
 186 primitives and variable program lengths, forcing the model to learn reusable, abstract building blocks.  
 187 This approach stands in contrast to methods like LPNs, which are limited to representing entire  
 188 programs in a single monolithic embedding.  
 189

190 The execution process is detailed in Algorithm 1. An initial state is created by embedding the input  
 191 query  $x_q$ . This state is then refined over  $T$  steps in a loop, where at each step  $t$ , the executor  $d_\theta$   
 192 uses the current program token  $z_t$  to compute an updated state. A crucial feature is the skip-token  
 193 gating mechanism: the probability of the skip token,  $\pi_t[\text{skip\_idx}]$ , is taken from the encoder's output  
 194 and used to linearly interpolate between the previous state  $s_{t-1}$  and the newly computed state. This  
 195 allows the model to effectively ignore an instruction  $z_t$ . After the final token is processed, the last  
 196 state is used to generate the output.  
 197

---

### 198 Algorithm 1 Neural Language Interpreter (Decoder $p_\theta$ )

---

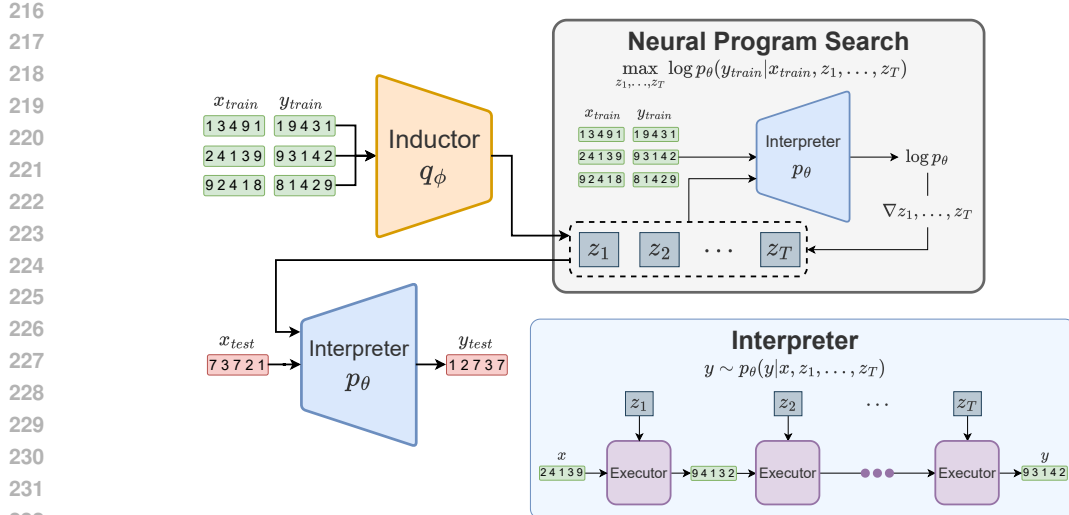
```

199 1: function  $p_\theta(y_q | x_q, z, \tau_d, h)$ 
200 2:    $(E, d, \text{MLP}) \leftarrow \theta$                                  $\triangleright$  Unpack implicit parameters from  $\theta$ 
201 3:    $s_0 \leftarrow \text{Embed}(x_q, E)$                                  $\triangleright$  Embed input
202 4:   for  $t = 1 \rightarrow T$  do
203 5:      $k_t \leftarrow d(s_{t-1}, z_{t-1})$                                  $\triangleright$  Transform state
204 6:      $l_t \leftarrow \text{MLP}(k_t)$                                  $\triangleright$  Project hidden state to logits
205 7:      $\pi_t \leftarrow \text{softmax}((l_t + h_t)/\tau_d)$                  $\triangleright$  Apply Gumbel-Softmax ( $h_t$  is Gumbel noise)
206 8:      $o_t \leftarrow E^\top \pi_t$                                  $\triangleright$  Compute new potential state
207 9:      $s_t \leftarrow \pi_t[\text{skip\_idx}] \cdot s_{t-1} + (1 - \pi_t[\text{skip\_idx}]) \cdot o_t$      $\triangleright$  Update state with skip-gating
208 10:   end for
209 11:    $l_y \leftarrow \text{MLP}(k_T)$                                  $\triangleright$  Generate final output logits
210 12:   return  $\text{softmax}(l_y)$ 
211 13: end function
212
213
```

---

## 213 4.3 SEARCHING NEURAL PROGRAMS

214 A key benefit of our model is the ability to refine an initial program prediction at test time using  
 215 gradient-based search. While the encoder provides a fast first guess, it may not be optimal, especially



270 

## 5 EXPERIMENTS

272 We evaluate NLI’s compositional generalisation capabilities across a custom diagnostic benchmark  
 273 for compositional generalisation and the compositionality version of the DeepCoder benchmark  
 274 (Balog et al., 2016), introduced in (Shi et al., 2023), comparing to a range of neural and neuro-  
 275 symbolic baselines.

277 **Benchmarks** The custom suite uses fixed-length sequences (20) and is designed to reveal failure  
 278 modes in PBE, where models see only input–output pairs. It comprises three splits containing different  
 279 tasks: *Shift-L*, training on small sequence shifts  $k \in \{1, \dots, 5\}$  and testing on larger unseen shifts  
 280  $k \in \{6, \dots, 10\}$ ; *Shift-P*, the inverse, training on large shifts  $k \in \{7, 8, 9\}$  and testing on smaller  
 281 ones  $k \in \{1, 2, 3\}$ ; and *Comp-I*, where models trained on single primitives (e.g.,  $f(x)$  or  $g(x)$ ) must  
 282 compose them at test time (e.g.,  $f(g(x))$ ). We also explore the compositionality deepcoder dataset  
 283 that scales the number of primitives and program complexity, see appendix A.

284 **Baselines and Models** We compare NLI against several strong baselines: In-Context Learning  
 285 (ICL), Test-Time Training (TTT), Latent Program Networks (LPN), and a discrete variant (D-LPN).  
 286 We evaluate three inference strategies for our model: Base Inference (direct encoder output), Prior  
 287 Search (sampling from the encoder), and our primary method, Gradient Search, which optimises the  
 288 program in the latent space.

290 

### 5.1 COMPOSITIONAL GENERALISATION IN NEURAL MODELS

293 Table 1: Performance for different methods and datasets, in the custom suite. We report final accuracy  
 294 for both in-distribution and out-of-distribution test splits (ID and OOD).

295 296 297 Method	298 Shift-L		299 Shift-P		300 Comp-I	
	301 ID	302 OOD	303 ID	304 OOD	305 ID	306 OOD
In-Context	1.00	0.00	1.00	0.00	1.00	0.13
TTT	1.00	0.00	1.00	0.00	0.95	0.14
LPN	1.00	0.00	1.00	0.00	1.00	0.18
LPN Gradient Search	1.00	0.03	1.00	0.00	1.00	0.29
D-LPN	1.00	0.02	1.00	0.00	0.99	0.15
D-LPN Gradient Search	1.00	0.01	1.00	0.00	0.99	0.20
NLI	1.00	0.00	1.00	0.00	1.00	0.17
NLI Prior Search	1.00	0.10	1.00	0.00	1.00	0.23
NLI Gradient Search	1.00	<b>0.99</b>	1.00	<b>1.00</b>	1.00	<b>0.91</b>

308 We train all models for 100k batches of size 512 and evaluate on held-out test splits, in- and out-of-  
 309 distribution. Due to the inference cost differences between NLI and baselines, for completeness, for  
 310 all baselines we also performed training runs with matched compute by increasing decoder layers,  
 311 for all baselines; this led to a degradation of in-distribution performance and no generalisation. We  
 312 report the higher, low inference 2-layer decoder results in table 1.

313 All models achieve near-perfect accuracy on the in-distribution (ID) test sets, demonstrating their  
 314 ability to solve tasks similar to those seen during training with neural induction. On the more  
 315 challenging out-of-distribution (OOD) splits, however, all baselines and the non-search variants of  
 316 our model fail to generalise. In-Context Learning (ICL) and the Latent Program Network (LPN and  
 317 D-LPN) show near 0% OOD accuracy on the shift tasks (Shift-L and Shift-P). Search-based LPNs  
 318 achieve only minor gains on Compose Isolation (Comp-I), but still fail to solve the task. In contrast,  
 319 NLI with Gradient Search exhibits strong compositional generalisation across all three benchmarks:  
 320 on Shift-L (length generalisation) it reaches 99% by extrapolating from small to larger unseen shifts;  
 321 on Comp-I (composing concepts) it achieves 91% by synthesising programs such as  $f(g(x))$ ; and  
 322 on Shift-P (primitive extraction) it attains a perfect 100% by “decompiling” primitives after training  
 323 only on complex ones. These results confirm that NLI achieves systematic generalisation, enabled  
 by gradient-based search, whereas the base encoder and prior search variants have performance in

324 line with In-Context, TTT and LPN baselines, which achieve no generalisation. The learned codes  
 325 further reveal systematic reuse of primitives. The model consistently represents a single left shift  
 326 with token 231 and a two-step shift with token 476, constructing larger programs by combining these  
 327 two building blocks. The OOD case of eight shifts is also expressed as a mixture of these primitives  
 328 (found via gradient search), highlighting how generalisation arises from recombination rather than  
 329 memorisation.

330

331

### 332 5.1.1 LEARNED PROGRAM REPRESENTATIONS

333

334 We study the task of shifting sequences to the left. During training, the model observes shifts of  
 335 length 1 to 5 (inclusive). In principle, the network could learn a separate token for each shift. Instead,  
 336 it discovers a more efficient representation by reusing tokens. Specifically, it learns a token (231) that  
 337 corresponds to a single left shift. By repeating this token, the network composes shifts of lengths 2  
 338 and 3. For larger shifts, it introduces a second token (476) corresponding to a two-step shift. This  
 339 enables the model to combine primitives to generate more complex shifts. For example, a shift of 4 is  
 340 represented as one two-step shift plus two one-step shifts. At test time, when generalising OOD to  
 341 larger shifts, the model composes primitives in the same manner. For instance, to represent an 8-step  
 342 shift, it uses four single-shift tokens and two two-shift tokens. This demonstrates both compression  
 343 (a small set of primitives) and compositionality (systematic reuse of primitives).

344

345

#### 346 Learned Program Representations for Shift-L

347

Ground Truth Program	NLI Program Representation
shift_left(1)	231
shift_left(2)	231 231
shift_left(3)	231 231 231
shift_left(4)	231 476 231
shift_left(5)	231 476 476
...	
shift_left(8) (OOD)	231 231 231 231 476 476

352

353

## 354 5.2 UNDERSTANDING THE ORIGINS OF NLI’S GENERALISATION CAPABILITIES

355

356

357 To investigate the origins of NLI’s generalisa-  
 358 tion, we conduct an ablation study across the  
 359 datasets in table 1, with results shown in fig. 2.  
 360 The base model achieves nearly perfect OOD ac-  
 361 curacy (97%), and we remove components indi-  
 362 vidually to assess their importance. Most prove  
 363 indispensable: dropping recurrent execution or  
 364 the discreteness of either program or layer repre-  
 365 sentations collapses OOD accuracy to near zero  
 366 (1–5%). This shows that discrete programs, dis-  
 367 crete layer traces, and recurrent dynamics are all  
 368 essential for generalisation. Dropping the skip  
 369 token reduces performance to 24%, consistent  
 370 with the model’s ability to learn its own skip, but  
 371 benefits from a dedicated token for faster, more  
 372 stable training. We also test the importance of  
 373 the encoder loss on performance, which results  
 374 in a small drop in performance. The benefit of  
 375 encoder loss can depend on the type of compo-  
 376 sitionality that is being tested. For example, it is useful for the type of composition in Shift-P, where  
 377 the underlying program primitives need to be represented to compose new programs that are shorter  
 378 than those seen during training. For length generalisation, where primitives that have already been  
 379 seen need to be combined into longer programs, the encoder loss does not affect performance.

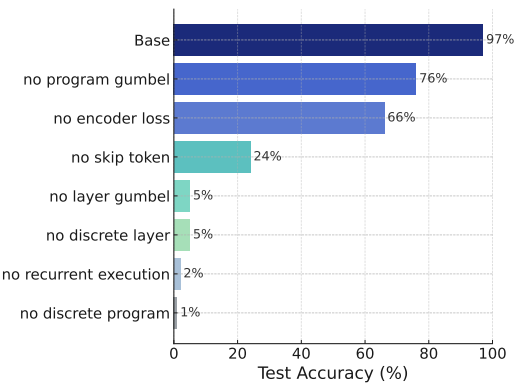


Figure 2: Ablations of the NLI base model to iden-  
 tify components critical for OOD generalisation.  
 For example, it is useful for the type of composition in Shift-P, where  
 the underlying program primitives need to be represented to compose new programs that are shorter  
 than those seen during training. For length generalisation, where primitives that have already been  
 seen need to be combined into longer programs, the encoder loss does not affect performance.

378  
379

## 5.3 GUMBEL-SOFTMAX

380  
381  
382  
383  
384  
385  
386  
387  
388

We also observe in fig. 2 that the Gumbel-Softmax relaxation, used to approximate discrete sampling, is a major driver of performance. Removing layer-level Gumbel sampling (*no layer gumbel*) causes near-complete failure on OOD compositional generalisation (dropping to 5%), while removing program-level Gumbel sampling (*no program gumbel*) reduces performance by 23 percentage points (to 76%). Although the encoder still outputs a distribution over a discrete codebook even without Gumbel-Softmax, we hypothesise that the network can still learn peaked distributions, allowing meaningful discrete representations to emerge naturally and preserving some degree of generalisation. However, explicitly adding the Gumbel-Softmax approximation significantly strengthens this inductive bias, leading to substantially better results.

389  
390  
391  
392  
393  
394  
395  
396  
397  
398

That said, our approach does not fundamentally depend on Gumbel-Softmax; any smooth relaxation of discrete sampling could be substituted (e.g., VQ-VAE with the straight-through estimator (van den Oord et al., 2017)). We chose Gumbel-Softmax primarily for its superior training stability. The straight-through estimator in VQ-VAE is known to suffer from biased gradients, codebook collapse (where many codebook entries remain unused, often requiring oversized codebooks or continual pruning) (Huh et al., 2023), and internal covariate shift between encoder outputs and codebook vectors (Łańcucki et al., 2020). Gumbel-Softmax is not without pitfalls either; stable training requires careful temperature scheduling. We find that annealing the temperature too quickly leads to severe performance degradation, as shown in our ablation on the Shift-L dataset (appendix C). With a gradual annealing schedule, however, training remains reliable and yields the strong results reported.

399

## 5.4 SCALING TEST-TIME PROGRAM SEARCH

400  
401  
402  
403  
404  
405  
406  
407  
408  
409  
410

To evaluate the effectiveness of our gradient-based search, we analyse how performance scales with the available computational budget at test time. We benchmark on the Comp-I dataset, varying two key hyperparameters: the number of parallel initialisations, Num starts, and the number of optimisation iterations, Gradient steps. The results, presented in fig. 3, demonstrate a strong and consistent positive correlation between test-time compute and final accuracy.

411  
412

## 5.5 DEEPCODER

413  
414  
415  
416

To assess the scalability of our approach, we evaluate NLI on the DeepCoder benchmark (Shi et al., 2023), a standard testbed for compositional generalisation in program synthesis.

417  
418  
419  
420  
421

**Dataset overview:** The DeepCoder dataset consists of short functional programs that manipulate lists of integers using a dedicated domain-specific language (DSL). Each program is a straight-line sequence of assignments. Every line defines a new variable by applying exactly one DSL operation to the input(s) or to previously defined variables, and the final variable is the program output.

422  
423  
424  
425

The DSL includes first-order operations (Head, Last, Take, Drop, Access, Minimum, Maximum, Reverse, Sort, Sum, etc.) as well as higher-order functionals (Map, Filter, Count, ZipWith, Scanl1) that accept one of a small fixed set of lambda expressions (e.g.,  $+1$ ,  $*2$ ,  $(-)$ ,  $>0$ , squaring, etc.).

426  
427  
428

For example, the program  $x0 = \text{INPUT} \rightarrow x1 = \text{Map}(x2) \ x0 \rightarrow x2 = \text{Filter}(>0) \ x1 \rightarrow x3 = \text{Sort} \ x2 \rightarrow x4 = \text{Reverse} \ x3$  applied to the input list  $[-2, 5, 0, 3, -1]$  yields the sorted positive doubled values  $[10, 6]$  as output.

429  
430  
431

We note that the original training datasets for DeepCoder composition have not been made public; therefore, data generation was run from scratch to generate datasets of size 11.6 million induction tasks, to train the neural baselines (NLI, LPN and In-context). Due to the prohibitive costs of the data sampling function, this is less than the 60 million used in the original work; however, baselines all

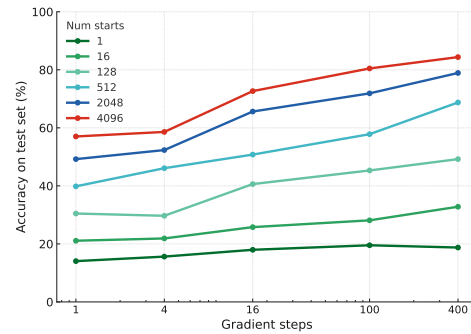


Figure 3: Performance on Compose-I, scaling two axes of test-time compute: gradient steps and number of starts.

achieve competitive performance. We highlight that neuro-symbolic approaches all leverage access to ground-truth programs during training, where NLI and LPN do not require this. However, adding program representations during training can serve as a powerful training signal for the neural decoders, which are otherwise bottlenecked by the encoder’s induction capacity. Therefore, for NLI and LPN, we add NLI w/ program and LPN w/ program baselines. These leverage an additional encoder mapping from program representations to latent space, resulting in an additional reconstruction loss, which is simply added to the total loss with equal weight to the standard encoder reconstruction loss. We give a complete description of the program encoder and our training procedure in appendix D. In contrast, NLI, along with neural baselines such as LPN, and an In-context baseline, must induce program behaviour solely from input-output pairs. All neural benchmarks were trained for 200k batches of size 512, see appendix B for more details. We find that end-to-end neural methods such as

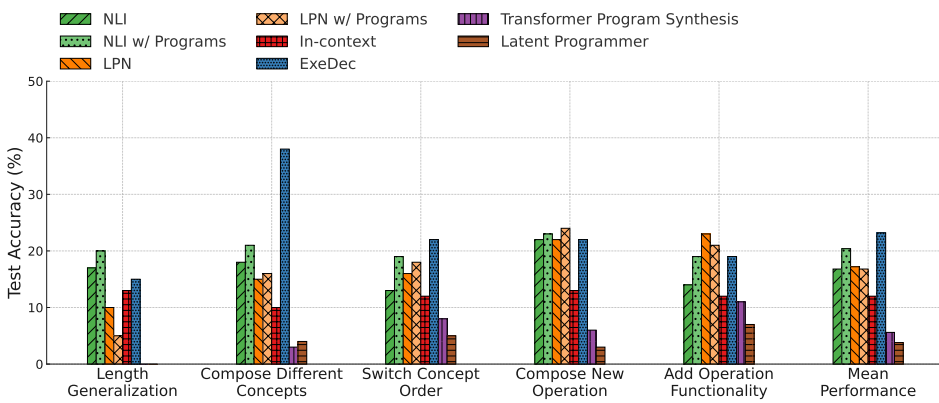


Figure 4: Comparison of fully neural baselines and NLI against neuro-symbolic methods. Neuro-symbolic models (ExeDec, Transformer, Latent Programmer) use ground-truth program annotations, while neural models (In-context, LPN, NLI) rely only on input–output pairs.

NLI and LPN substantially outperform earlier Latent Programmer approaches and Transformer-based program synthesis. Secondly, despite the absence of program supervision, they achieve performance competitive with ExeDec (Shi et al., 2023), highlighting the capacity of neural PBE approaches to autonomously discover structured program representations.

A direct comparison between NLI and LPN further reveals complementary strengths. NLI generalises more effectively to longer programs and novel concept compositions, which is a particular strength of NLI due to its ability to compose programs of arbitrary length. In contrast, LPN excels at switching concept order and extending functionality with new operations. These differences suggest that their learned latent structures capture distinct inductive biases, leading to different generalisation behaviours out of distribution.

## 6 RELATED WORK

**Symbolic Program Synthesis.** Early work in program synthesis largely relied on symbolic techniques and DSLs. Classical systems, such as those by Summers (1977) and Gulwani (2011), used predefined DSLs with explicit search over symbolic programs. These methods provide interpretability and exactness but suffer from scalability issues, as every new domain requires manual DSL design. Recent neuro-symbolic hybrids, such as DeepCoder (Balog et al., 2016), combine a neural predictor with symbolic search, predicting program components to accelerate search. However, their reliance on restricted DSLs limits generalisation beyond the designed primitives.

**Neural Program Induction and Meta Learning** Neural approaches aim to overcome the brittleness of symbolic methods by learning programs directly from examples. Neural Programmer-Interpreters (Reed & De Freitas, 2016) execute programs implicitly with recurrent models, while Devlin et al. (2017) introduced meta-induction for few-shot learning. These models improve adaptability but often fail to generalise compositionally and demand large supervision. ExeDec (Shi et al., 2023) added execution decomposition as an inductive bias, yet still relies on ground-truth decompositions and

486 remains costly. Meta learning advances this by training networks to adapt across task distributions  
 487 (Finn et al., 2017), a setup closely related to the optimisation considered here.  
 488

489 **Latent Representations of Programs.** Another line of work introduces latent spaces to represent  
 490 programs more flexibly. CompILE (Kipf et al., 2018) segments demonstrations into reusable latent  
 491 codes with Gumbel-Softmax relaxation, showing benefits for imitation learning. The Latent Pro-  
 492 grammer (Hong et al., 2020) extends this idea to discrete latent codes that plan over input–output  
 493 examples, using a VQ-VAE style autoencoder with beam search in latent space, see appendix E for a  
 494 discussion on its relation to NLI. Most recently, Latent Program Networks (LPNs) (Macfarlane &  
 495 Bonnet, 2024) proposed continuous latent program representations to facilitate test-time search, but  
 496 the lack of discrete compositional structure hinders combinatorial generalisation.  
 497

498 **Compositionality and Generalisation.** Compositional generalisation remains a central challenge  
 499 in neural program synthesis. Lake & Baroni (2018) demonstrated that standard seq2seq models  
 500 fail to generalise systematically to novel compositions. Approaches such as the Compositional  
 501 Recursive Learner (CRL) (Chang et al., 2019) attempt to address this by learning to compose reusable  
 502 transformations. Similarly, recursion-based methods (Cai et al., 2017) leverage inductive biases  
 503 from programming languages to handle inputs of greater complexity than those seen during training.  
 504 While these directions highlight the importance of compositional structure, they either rely on strong  
 505 supervision or achieve only limited scalability.  
 506

507 **Discrete Representation Learning.** Discrete latent representations provide a natural way to capture  
 508 compositional structure and improve interpretability. The Vector-Quantized Variational Autoencoder  
 509 (VQ-VAE) (van den Oord et al., 2017) exemplifies this approach by learning a finite codebook of  
 510 tokens, with gradients passed via a straight-through estimator. A complementary method is the  
 511 Gumbel-Softmax relaxation (Jang et al., 2017), which reparameterizes categorical sampling with a  
 512 differentiable approximation. Together, these techniques enable end-to-end training with discrete  
 513 variables while retaining symbolic structure. A practical example arises in hierarchical reinforcement  
 514 learning, where the options framework (Sutton et al., 1999) defines a set of reusable, temporally  
 515 extended actions that compose into complex behaviours. Such discrete units, whether tokens in  
 516 generative models or skills in RL, form compact and interpretable building blocks that support  
 517 compositional generalisation and long-horizon reasoning.  
 518

## 519 7 CONCLUSION

520 In this work, we introduced the Neural Language Interpreter (NLI), a novel architecture that bridges  
 521 the divide between symbolic and neural approaches in program synthesis. By learning a discrete,  
 522 symbolic-like language and a differentiable interpreter, NLI combines the compositional strengths  
 523 of symbolic systems with the flexibility of neural networks. The model discovers a vocabulary of  
 524 primitive operations and composes them into variable-length programs, refined at test time through  
 525 efficient gradient-based search. Our evaluations show that NLI outperforms existing methods on  
 526 challenging compositional generalisation tasks, with ablations confirming that the discrete, sequential  
 527 program representation is key to this success.  
 528

529 **Limitations and Future Work:** NLI introduces a new paradigm for program induction that demon-  
 530 strates promising compositional generalisation. While we believe it has strong potential to scale to  
 531 significantly harder problems, the present work is an initial exploration and naturally comes with  
 532 several limitations that highlight exciting directions for future research. A primary bottleneck is  
 533 the computational cost of test-time search in the latent representation space; although NLI proves  
 534 remarkably robust to overfitting even under constrained search budgets, scaling to more complex tasks  
 535 will likely require more efficient inference strategies, with evolutionary/local search being promising  
 536 directions. As problem difficulty increases, programs will grow both in length and vocabulary size,  
 537 potentially leading to vanishing or exploding gradients, which, while not observed in our experiments,  
 538 could require architectural modifications at scale. The current interpreter also limits expressive power:  
 539 each layer conditions on exactly one token, preventing parameterised primitives (e.g., `add(k)` for  
 540 variable  $k$ ), and execution follows a strictly sequential flow without conditional branching.  
 541

## 542 REFERENCES

543 Saqib Ameen and Levi H. S. Lelis. Program synthesis with best-first bottom-up search. *Journal of*  
 544 *Artificial Intelligence Research*, 77:1271–1310, 2023. doi: 10.1613/jair.1.14394.  
 545

540 Matej Balog, Alexander L Gaunt, Marc Brockschmidt, Sebastian Nowozin, and Daniel Tarlow.  
 541 Deepcoder: Learning to write programs. *arXiv preprint arXiv:1611.01989*, 2016.  
 542

543 Shraddha Barke, Hila Peleg, and Nadia Polikarpova. Just-in-time learning for bottom-up enumerative  
 544 synthesis. In *Proceedings of the ACM on Programming Languages*, volume 4, pp. 1–29, 2020.

545 Marco Baroni. Linguistic generalization and compositionality in modern artificial neural networks.  
 546 *Philosophical Transactions of the Royal Society B*, 375(1791):20190307, 2020.

547 Jonathon Cai, Richard Shin, and Dawn Song. Making neural programming architectures generalize  
 548 via recursion. *arXiv preprint arXiv:1704.06611*, 2017.

549 Michael Chang, Abhishek Gupta, Sergey Levine, and Thomas L Griffiths. Automatically composing  
 550 representation transformations as a means for generalization. In *International Conference on  
 551 Learning Representations (ICLR)*, 2019.

552 Jacob Devlin, Jonathan Uesato, Rishabh Bhupatiraju, Rishabh Singh, Abdel-rahman Mohamed, and  
 553 Pushmeet Kohli. Neural program meta-induction. In *Advances in Neural Information Processing  
 554 Systems (NeurIPS)*, 2017.

555 Chelsea Finn, Pieter Abbeel, and Sergey Levine. Model-agnostic meta-learning for fast adaptation of  
 556 deep networks. In *International conference on machine learning*, pp. 1126–1135. PMLR, 2017.

557 Sumit Gulwani. Automating string processing in spreadsheets using input-output examples. *ACM  
 558 Sigplan Notices*, 46(1):317–330, 2011.

559 David Ha and Jürgen Schmidhuber. Recurrent world models facilitate policy evolution. *Advances in  
 560 neural information processing systems*, 31, 2018.

561 Jason Hong, Maxwell Nye, Joshua B Tenenbaum, and Charles Sutton. Latent programmer: Discrete  
 562 latent codes for program synthesis. In *Advances in Neural Information Processing Systems  
 563 (NeurIPS)*, 2020.

564 Holger H. Hoos and Thomas Stützle. *Stochastic Local Search: Foundations and Applications*.  
 565 Elsevier/Morgan Kaufmann, 2004.

566 Minyoung Huh, Brian Cheung, Pulkit Agrawal, and Phillip Isola. Straightening out the straight-  
 567 through estimator: Overcoming optimization challenges in vector quantized networks. In *Interna-  
 568 tional Conference on Machine Learning*, pp. 14096–14113. PMLR, 2023.

569 Idress Husien and Sven Schewe. Program generation using simulated annealing and model checking.  
 570 In Rocco De Nicola and Eva Kühn (eds.), *Software Engineering and Formal Methods*, pp. 155–171,  
 571 2016. ISBN 978-3-319-41591-8.

572 Eric Jang, Shixiang Gu, and Ben Poole. Categorical reparameterization with gumbel-softmax. In  
 573 *International Conference on Learning Representations (ICLR)*, 2017.

574 Thomas Kipf, Ethan Li, Hanjun Dai, Zornitsa Kozareva, Jiaming Song, Arvind Neelakantan, and Max  
 575 Welling. Compile: Compositional imitation learning and execution. In *International Conference  
 576 on Machine Learning (ICML)*, 2018.

577 Brenden Lake and Marco Baroni. Generalization without systematicity: On the compositional skills  
 578 of sequence-to-sequence recurrent networks. In *International conference on machine learning*, pp.  
 579 2873–2882. PMLR, 2018.

580 Adrian Łaćucki, Jan Chorowski, Guillaume Sanchez, Ricard Marxer, Nanxin Chen, Hans JGA  
 581 Dolfig, Sameer Khurana, Tanel Alumäe, and Antoine Laurent. Robust training of vector quantized  
 582 bottleneck models. In *2020 International Joint Conference on Neural Networks (IJCNN)*, pp. 1–7.  
 583 IEEE, 2020.

584 Matthew V Macfarlane and Clément Bonnet. Searching latent program spaces. *arXiv preprint  
 585 arXiv:2411.08706*, 2024.

586 Chris J Maddison, Andriy Mnih, and Yee Whye Teh. The concrete distribution: A continuous  
 587 relaxation of discrete random variables. *arXiv preprint arXiv:1611.00712*, 2016.

594 Augustus Odena, Kensen Shi, David Bieber, Rishabh Singh, Charles Sutton, and Hanjun Dai.  
595 BUSTLE: Bottom-up program synthesis through learning-guided exploration. In *International*  
596 *Conference on Learning Representations*, 2021.

597

598 Scott Reed and Nando De Freitas. Neural programmer-interpreters. In *International Conference on*  
599 *Learning Representations (ICLR)*, 2016.

600 Quazi Asif Sadmine, Hendrik Baier, and Levi Lelis. Language models speed up local search  
601 for finding programmatic policies. *Transactions on Machine Learning Research*, 2024. ISSN  
602 2835-8856.

603

604 Zhi Shi, Maxwell Nye, Rudy Bunel, Rishabh Singh, Pushmeet Kohli, and Alexander L Gaunt.  
605 Exedec: Execution decomposition for compositional generalization in neural program synthesis.  
606 In *Advances in Neural Information Processing Systems (NeurIPS)*, 2023.

607 Armando Solar-Lezama, Rodric Rabbah, Rastislav Bodík, and Martin Rinard. Combinatorial  
608 sketching for finite programs. In *Computer Aided Verification*, volume 4144 of *Lecture Notes in*  
609 *Computer Science*, pp. 404–420. Springer, 2006.

610 Phillip D Summers. A methodology for lisp program construction from examples. *Journal of the*  
611 *ACM (JACM)*, 24(1):161–175, 1977.

612

613 Richard S Sutton, Doina Precup, and Satinder Singh. Between mdps and semi-mdps: A framework  
614 for temporal abstraction in reinforcement learning. *Artificial intelligence*, 112(1-2):181–211, 1999.

615 Aaron van den Oord, Oriol Vinyals, and Koray Kavukcuoglu. Neural discrete representation learning.  
616 In *Advances in Neural Information Processing Systems*, 2017.

617

618

619

620

621

622

623

624

625

626

627

628

629

630

631

632

633

634

635

636

637

638

639

640

641

642

643

644

645

646

647

648  
649

## A DATASETS

650  
651

## A.1 COMPOSITIONALITY BENCHMARK

652  
653  
654  
655

We constructed the Compositionality Benchmark using our own sampling and problem synthesis procedures to evaluate distinct facets of compositional reasoning. The benchmark comprises three main tasks designed to probe different dimensions of generalisation. For each task, dataset sizes were chosen to provide a robust training scale and sufficient evaluation coverage. The three splits are:

656

1. **Permutation Length Generalisation (Shift-L).** This task measures extrapolation on a parameterized function. The model learns a `left_shift(n)` operation on a sequence. Training is restricted to a small, contiguous range of integer shifts, specifically for  $n \in \{1, 2, 3, 4, 5\}$ . Evaluation is performed on larger, unseen shift values,  $n \in \{6, 7, 8, 9, 10\}$ . This measures the model’s ability to generalise beyond the magnitude of parameters observed during training.
2. **Sub-Function Extraction (Shift-P).** This task tests whether a model can infer a general, parameterized function from sparse and non-contiguous examples. The underlying operation is again `left_shift(n)`. Training is performed on a sparse set of non-adjacent shift values (e.g.,  $n \in \{5, 7, 9\}$ ). Evaluation then probes generalisation to a different, unseen range of values (e.g.,  $n \in \{1, 2, 3\}$ ), testing whether the model has learned the abstract concept of “shifting by  $n$ ” rather than memorizing separate programs for each training example.
3. **Composition of Primitives (Comp-I).** This task evaluates whether a model can compose primitive functions it has only seen in isolation. The model is provided with a library of over 20 primitive sequence-to-sequence operations (e.g., `reverse`, `shift_left_3`, `increment_2`). During training, the model only sees programs consisting of a single primitive operation. For evaluation, it must execute programs that are compositions of two or more primitives, testing for generalisation from individual operations to novel compositions.

657  
658  
659  
660  
661  
662  
663  
664  
665  
666  
667  
668669  
670  
671  
672  
673  
674  
675  
676

Table 2: Dataset sizes for the Compositionality Benchmark.

677  
678  
679  
680  
681  
682  
683

## A.2 DEEPCODER

684  
685  
686  
687  
688

We use the DeepCoder domain and adopt the compositional generalisation splits from the ExeDec codebase Shi et al. (2023). Following their Domain-Specific Language (DSL) and splitting procedures, we sampled 2,000,000 training tasks and 10,000 test tasks. The five splits are designed to probe different dimensions of compositional generalisation:

689  
690  
691  
692  
693  
694  
695  
696  
697  
698  
699  
700  
701

1. **Length-Generalisation.** Training programs contain 1–4 lines, while test programs have length 5. This evaluates whether models can extrapolate to deeper compositions than observed during training Balog et al. (2016).
2. **Compose-Different-Concepts.** Operations are partitioned into two groups: (i) all first-order operations plus `Map`, and (ii) all remaining higher-order operations. Training only composes within a single group, while test programs require mixing across groups. This measures cross-concept compositionality.
3. **Switch-Concept-Order.** Training tasks always compose operations in a fixed group ordering (e.g., first-order → higher-order), while test tasks reverse the ordering. This evaluates whether models can generalise to new sequential structures of concepts.
4. **Compose-New-Operation.** The held-out operation is `Scan11`. Training tasks either use `Scan11` in isolation (25% of tasks) or exclude it entirely, while test tasks require `Scan11` to be composed with other operations. This probes whether the model can generalise an operator from isolated usage to composed contexts.

702  
703 5. **Add-Operation-Functionality.** Training only uses Scan11 with lambdas (–) and min.  
704 Test tasks require Scan11 with new lambdas (+), (×), and max. This tests whether models  
705 can extend their understanding of a known operator by analogy to other operations.  
706

707 Table 3: Dataset sizes for DeepCoder, generated using the ExeDec repository.  
708

Split	Size
Train	11,600,000
Test	10,000

712  
713  
714  
715  
716  
717  
718  
719  
720  
721  
722  
723  
724  
725  
726  
727  
728  
729  
730  
731  
732  
733  
734  
735  
736  
737  
738  
739  
740  
741  
742  
743  
744  
745  
746  
747  
748  
749  
750  
751  
752  
753  
754  
755

756 **B HYPERPARAMETERS**  
757  
758759 Table 4: Model Hyperparameters for NLI. The same default configuration was used across all datasets.  
760

761 <b>Hyperparameter</b>	762 <b>Shift-L</b>	763 <b>Shift-P</b>	764 <b>Compose I</b>	765 <b>DeepCoder</b>
<b>Model Architecture</b>				
766 Model Dimension ( $d_{\text{model}}$ )	128	128	128	128
767 Number of Heads ( $n_{\text{head}}$ )	8	8	8	8
768 Feed-Forward Dimension ( $d_{\text{ff}}$ )	512	512	512	512
769 Encoder Layers	2	2	2	4
770 Decoder Layers	2	2	2	2
771 Positional Embedding	Sinusoidal	Sinusoidal	Sinusoidal	Sinusoidal
772 Gradient Clip Norm	2.0	2.0	2.0	2.0
<b>Program Generation</b>				
773 Program Vocabulary Size	512	512	512	512
774 Program Length (Training)	10	10	4	4
<b>Training</b>				
775 Learning Rate	2e-4	2e-4	2e-4	2e-4
776 Num Batches	100k	100k	100k	200k
<b>Gumbel-Softmax Sampling (Program)</b>				
777 Use Program Gumbel	True	True	True	True
778 Start Temperature	8.0	8.0	8.0	8.0
779 End Temperature	0.5	0.5	0.5	0.5
780 Annealing Batches	20,000	20,000	100,000	200,000
781 Decay Strategy	Exponential	Exponential	Exponential	Exponential
782 Straight-Through	False	False	False	False
<b>Gumbel-Softmax Sampling (Decoder Layer)</b>				
783 Use Layer Gumbel	True	True	True	True
784 Start Temperature	2.0	2.0	2.0	2.0
785 End Temperature	0.5	0.5	0.5	0.5
786 Annealing Batches	20,000	20,000	100,000	200,000
787 Decay Strategy	Exponential	Exponential	Exponential	Exponential
788 Straight-Through	False	False	False	False
<b>Regularization &amp; Losses</b>				
789 Encoder Loss Coefficient	0.00001	0.00001	0.00001	0.00001
<b>Search</b>				
790 Gradient Steps	100	100	100	100
791 Number of Initializations	1024	1024	8192	1024
792 Std for initialisation	7.5	7.5	7.5	7.5

810  
 811  
 812  
 813  
 814  
 815  
 816  
 817  
 818  
 819  
 820  
 821  
 822  
 823  
 824  
 825  
 826  
 827

828 Table 5: Model Hyperparameters for LPN. The same default configuration was used across all  
 829 datasets.

Hyperparameter	Shift-L	Shift-P	Compose I	DeepCoder
<b>Model Architecture</b>				
Model Dimension ( $d_{\text{model}}$ )	512	512	512	512
Number of Heads ( $n_{\text{head}}$ )	8	8	8	8
Feed-Forward Dimension ( $d_{\text{ff}}$ )	512	512	512	512
Encoder Layers	2	2	2	4
Decoder Layers	2	2	2	2
Use Layer Normalization	True	True	True	True
Positional Embedding	Sinusoidal	Sinusoidal	Sinusoidal	Sinusoidal
Dropout Rate	0.0	0.0	0.0	0.0
VAE Beta ( $\beta$ )	0.001	0.001	0.001	0.001
Gradient Clip Norm	2.0	2.0	2.0	2.0
<b>Training</b>				
Learning Rate	2e-4	2e-4	2e-4	2e-4
Num Batches	100k	100k	100k	200k

848  
 849  
 850  
 851  
 852  
 853  
 854  
 855  
 856  
 857  
 858  
 859  
 860  
 861  
 862  
 863

864  
865  
866  
867  
868  
869  
870  
871

872 Table 6: Model Hyperparameters for D-LPN. The same default configuration was used across all  
873 datasets.

Hyperparameter	Shift-L	Shift-P	Compose I
<b>Model Architecture</b>			
Model Dimension ( $d_{\text{model}}$ )	512	512	512
Number of Heads ( $n_{\text{head}}$ )	8	8	8
Feed-Forward Dimension ( $d_{\text{ff}}$ )	512	512	512
Encoder Layers	2	2	2
Decoder Layers	2	2	2
Use Layer Normalization	True	True	True
Positional Embedding	Sinusoidal	Sinusoidal	Sinusoidal
Dropout Rate	0.0	0.0	0.0
Gradient Clip Norm	2.0	2.0	2.0
<b>Training</b>			
Learning Rate	2e-4	2e-4	2e-4
Num Batches	100k	100k	100k
<b>Gumbel-Softmax Sampling (Program)</b>			
Use Program Gumbel	True	True	True
Start Temperature	8.0	8.0	8.0
End Temperature	0.5	0.5	0.5
Annealing Batches	20,000	20,000	100,000
Decay Strategy	Exponential	Exponential	Exponential
Straight-Through	False	False	False
<b>Gumbel-Softmax Sampling (Decoder Layer)</b>			
Use Layer Gumbel	True	True	True
Start Temperature	2.0	2.0	2.0
End Temperature	0.5	0.5	0.5
Annealing Batches	20,000	20,000	100,000
Decay Strategy	Exponential	Exponential	Exponential
Straight-Through	False	False	False

911  
912  
913  
914  
915  
916  
917

918  
 919  
 920  
 921  
 922  
 923  
 924  
 925  
 926  
 927  
 928  
 929  
 930  
 931  
 932  
 933  
 934  
 935  
 936

Table 7: Model Hyperparameters for In-context. The same default configuration was used across all datasets.

Hyperparameter	Shift-L	Shift-P	Compose I	DeepCoder
<b>Model Architecture</b>				
Model Dimension ( $d_{\text{model}}$ )	512	512	512	512
Number of Heads ( $n_{\text{head}}$ )	8	8	8	8
Feed-Forward Dimension ( $d_{\text{ff}}$ )	512	512	512	512
Encoder Layers	2	2	2	4
Decoder Layers	2	2	2	2
Use Layer Normalization	True	True	True	True
Positional Embedding	Sinusoidal	Sinusoidal	Sinusoidal	Sinusoidal
Dropout Rate	0.0	0.0	0.0	0.0
Gradient Clip Norm	2.0	2.0	2.0	2.0
<b>Training</b>				
Learning Rate	2e-4	2e-4	2e-4	2e-4
Num Batches	100k	100k	100k	200k

955  
 956  
 957  
 958  
 959  
 960  
 961  
 962  
 963  
 964  
 965  
 966  
 967  
 968  
 969  
 970  
 971

972 C GUMBEL-SOFTMAX TEMPERATURE ANNEALING ABLATION  
973974 In this section, we investigate how the base NLI model learns discrete program representations under  
975 different Gumbel-Softmax temperature annealing schedules. Stable training requires careful control  
976 of the program- and layer-level temperatures, and here we ablate the effect of the shared annealing  
977 duration on the Shift-L dataset.978 Our model uses two independent Gumbel-Softmax temperatures:  
979980 

- 981 • **Program temperature** ( $\tau_{\text{prog}}$ ): controls the discreteness of the tokenised high-level program.
- 982 • **Layer temperature** ( $\tau_{\text{layer}}$ ): controls the discreteness of per-token execution choices within  
983 each layer.

984 Both temperatures are linearly annealed over the same number of steps ( $\tau_{\text{prog}}$ : 4.0→0.5,  $\tau_{\text{layer}}$ :  
985 2.0→0.5), after which they are held fixed at 0.5 for the remainder of training. All runs use 100k total  
986 training steps and identical hyperparameters, varying only the shared annealing duration.  
987988 Table 8: Ablation of the shared Gumbel-Softmax temperature annealing duration on Shift-L (in-  
989 distribution accuracy; 100k total training steps, averaged over 3 seeds).  
990

Annealing duration	NLI (ID)
1k steps	0.00
5k steps	0.41
10k steps	1.00
20k steps	1.00
50k steps	1.00
100k steps	1.00

991 Short annealing schedules (1k–5k steps) fail to produce stable discrete program representations.  
992 Accuracy increases sharply at 10k steps, after which all longer schedules perform identically. This  
993 shows that the model is robust to the exact duration once a minimal threshold is reached, and that our  
994 default 20k-step schedule lies well within the stable regime for Shift-L.  
995996 1003  
997 1004  
998 1005  
999 1006  
1000 1007  
1001 1008  
1002 1009  
1003 1010  
1004 1011  
1005 1012  
1006 1013  
1007 1014  
1008 1015  
1009 1016  
1010 1017  
1011 1018  
1012 1019  
1013 1020  
1014 1021  
1015 1022  
1016 1023  
1017 1024  
1018 1025

1026 **D PROGRAM ENCODER**  
10271028 In this section, we describe the program encoder used alongside the input–output (I/O) encoder. The  
1029 program encoder can be leveraged when data is available to provide a stronger, more direct training  
1030 signal to the neural executor. When training relies solely on the I/O encoder, the discrete program  
1031 latents can become bottlenecked by the encoder’s limited inductive capacity, particularly on harder  
1032 tasks. Providing ground-truth programs during training alleviates this issue and allows the executor  
1033 to learn the correct program primitives more effectively. Below, we outline the tokenisation scheme,  
1034 architecture, and training procedure.1035 **D.1 TOKENISATION**  
10361037 Programs are whitespace-tokenised according to the DeepCoder DSL. The full vocabulary contains  
1038 153 tokens: 4 special tokens (`PAD`, `<BOS>`, `<EOS>`, `|`), 4 structural tokens (`=`, `INPUT`, `[`, `]`), 15  
1039 operations, 19 lambda functions, 10 variable tokens `x0–x9`, and integer literals from  $-50$  to  $50$ .1040 **Example**  
10411042 **String representation:** `x0 = INPUT | x1 = Map (+1) x0 | x2 = Filter (>0) x1`  
1043 `| x3 = Head x2`  
10441045 **Token sequence (with `<BOS>` and `<EOS>`):** `<BOS> x0 = INPUT | x1 = Map (+1) x0 |`  
1046 `x2 = Filter (>0) x1 | x3 = Head x2 <EOS>`1047 **Tokenised sequence (token IDs):** 1 42 4 5 3 43 18 23 42 3 44 19 33 43 3 45 8  
1048 44 2  
10491050 **D.2 ARCHITECTURE**  
10511052 The program encoder uses the same architecture and hyperparameters as the I/O encoder in all  
1053 experiments. Both encoders share the same codebook and use Gumbel–Softmax relaxation to produce  
1054 discrete latent programs.1055 **D.3 TRAINING WITH THE PROGRAM ENCODER**  
10561057 Access to ground-truth programs  $P$  allows the model to bypass the inductive bottleneck of the I/O  
1058 encoder and directly expose the executor to correct program structures. We do not introduce a separate  
1059 program decoder; instead, both encoders share the neural execution decoder  $p_\theta$ .1060 During training, the program encoder maps each tokenised program  $P$  to discrete latents using the  
1061 shared codebook. The total objective adds an auxiliary reconstruction term weighted by  $\lambda_{\text{prog}}$ , which  
1062 we set to 1.0 in all experiments.

1063  
1064 
$$\mathcal{L}_{\text{rec}} = \mathcal{L}_{\text{IO\_rec}} + \lambda_{\text{prog\_rec}} \mathcal{L}_{\text{prog\_rec}}$$
  
1065

1066 To ensure both encoders learn a unified latent space, we control gradient flow as follows. Gradients  
1067 from  $\mathcal{L}_{\text{prog}}$  update both the program encoder parameters and the executor, whereas gradients from  
1068  $\mathcal{L}_{\text{IO}}$  do not update the executor (stop-gradient), forcing the I/O encoder to align with the program  
1069 encoder’s higher-quality latents.1070 At test time, the program encoder is discarded. Only the trained I/O encoder and executor are used  
1071 for inference and search.1072  
1073  
1074  
1075  
1076  
1077  
1078  
1079

1080 E COMPARISON TO DISCRETE LATENT PROGRAMMER  
10811082 We compare our model with the Discrete Latent Programmer (DLP) (Hong et al., 2020), which also  
1083 employs discrete latent codes for program induction. While both approaches share this high-level  
1084 similarity, they diverge substantially in their architectures, training assumptions, and mechanisms  
1085 for test-time adaptation. The key differences lie in how programs are executed and how search is  
1086 performed at inference.  
10871088 E.1 PROGRAM EXECUTION AND SUPERVISION  
10891090 In our model, program tokens are interpreted by a recurrent neural interpreter that applies each token  
1091 as an operation to an intermediate state. This sequential execution enables variable-length programs,  
1092 promotes compositional reuse of learned primitives, and allows the model to be trained end-to-end on  
1093 raw input–output examples alone. Since outputs can be directly compared to targets, no ground-truth  
1094 program annotations are required.  
10951096 DLP, by contrast, does not include a neural interpreter. Its decoder predicts full program sequences  
1097 from latent codes, and training requires access to the underlying program representations. This  
1098 reliance on program supervision restricts DLP to domains where the generating programs are known  
1099 and a domain-specific language is available, limiting its applicability beyond synthetic benchmarks.  
1100

## E.2 TEST-TIME PROGRAM SEARCH

A further distinction arises in test-time adaptation. Our model exploits the differentiability of the  
neural interpreter to refine latent program embeddings via gradient-based search. This procedure  
enables efficient adaptation: initial program guesses from the encoder can be continuously optimized  
to better fit new examples, even when they require novel compositions not seen during training.In contrast, DLP performs beam search in the discrete program space. This search is combinatorial,  
lacks gradient guidance, and cannot refine programs based on execution error. As a result, DLP’s  
generalisation is hindered, particularly in out-of-distribution settings where small corrections to a  
predicted program are necessary. By enabling gradient-based refinement in a relaxed latent space,  
our model provides a more powerful and adaptive mechanism for program synthesis.

1134 F NLI PROGRAM REPRESENTATIONS  
11351136 In this section, we provide examples of the discrete latent codes discovered by NLI, both for  
1137 in-distribution programs and for how these primitives are composed by search to generalise out-of-  
1138 distribution (OOD).  
11391140 F.1 SHIFT-L  
11411142 We study the task of shifting sequences to the left. During training, the model observes shifts of  
1143 length 1 to 5 (inclusive). In principle, the network could learn a separate token for each shift. Instead,  
1144 it discovers a more efficient representation by reusing tokens. Specifically, it learns a token (231) that  
1145 corresponds to a single left shift. By repeating this token, the network composes shifts of lengths 2  
1146 and 3. For larger shifts, it introduces a second token (476), which corresponds to a two-step shift.  
1147 This enables the model to combine primitives to generate more complex shifts.  
11481149 For example, a shift of 4 is represented as one two-step shift plus two one-step shifts. At test time,  
1150 when generalising OOD to larger shifts, the model composes primitives in the same manner. For  
1151 instance, to represent an 8-step shift, it uses four single-shift tokens and two two-shift tokens. This  
1152 demonstrates both compression (a small set of primitives) and compositionality (systematic reuse of  
1153 primitives).  
1154

```

1 -----
2
3 Example 1: Shift Left by 1
4
5 Task Specification:
6 Input: [8, 2, 5, 9, 1, 6, 3, 4, 7, 0]
7 Output: [2, 5, 9, 1, 6, 3, 4, 7, 0, 8]
8
9 Ground Truth Program: y = left_shift(x, 1)
10 NLI Program Representation: 231
11
12 -----
13
14 Example 2: Shift Left by 2
15
16 Task Specification:
17 Input: [4, 6, 7, 1, 9, 0, 3, 8, 5, 2]
18 Output: [7, 1, 9, 0, 3, 8, 5, 2, 4, 6]
19
20 Ground Truth Program: y = left_shift(x, 2)
21 NLI Program Representation: 231 231
22
23 -----
24
25 Example 3: Shift Left by 3
26
27 Task Specification:
28 Input: [3, 7, 4, 0, 6, 2, 9, 5, 8, 1]
29 Output: [0, 6, 2, 9, 5, 8, 1, 3, 7, 4]
30
31 Ground Truth Program: y = left_shift(x, 3)
32 NLI Program Representation: 231 231 231
33
34 -----
35
36 Example 4: Shift Left by 4
37
38 Task Specification:
39 Input: [5, 1, 9, 2, 8, 6, 0, 7, 3, 4]
40 Output: [8, 6, 0, 7, 3, 4, 5, 1, 9, 2]
41
42 Ground Truth Program: y = left_shift(x, 4)

```

```

1188 43 NLI Program Representation: 231 476 231
1189 44
1190 45 -----
1191 46
1192 47 Example 5: Shift Left by 5
1193 48
1194 49 Task Specification:
1195 50 Input: [9, 4, 1, 5, 2, 7, 6, 0, 3, 8]
1196 51 Output: [7, 6, 0, 3, 8, 9, 4, 1, 5, 2]
1197 52
1198 53 Ground Truth Program: y = left_shift(x, 5)
1199 54 NLI Program Representation: 231 476 476
1200 55
1201 56 -----
1202 57 Example 6 (OOD): Shift Left by 8
1203 58
1204 59 Task Specification:
1205 60 Input: [0, 1, 2, 3, 4, 5, 6, 7, 8, 9]
1206 61 Output: [8, 9, 0, 1, 2, 3, 4, 5, 6, 7]
1207 62
1208 63 Ground Truth Program: y = left_shift(x, 8)
1209 64 NLI Program Representation: 231 231 231 231 476 476
1210 65
1211 66 -----
1212 67

```

Listing 1: Learned NLI Program Representations for List Shift Tasks.

```

1213
1214
1215
1216
1217
1218
1219
1220
1221
1222
1223
1224
1225
1226
1227
1228
1229
1230
1231
1232
1233
1234
1235
1236
1237
1238
1239
1240
1241

```

---

## 1242 G APPENDIX: TOKEN REUSE REGULARISATION LOSS

1244 To bias the model toward learning a compact and reusable set of primitives, we introduce a regularisa-  
 1245 tion term applied to the encoder’s output distribution. Since the encoder generates the latent program  
 1246 representation, this regulariser directly shapes the structure of the learned latent space. We refer to  
 1247 this term as the *token reuse loss*. Its role is to discourage the encoder from spreading probability  
 1248 mass across too many distinct program tokens within a batch. By promoting reuse, the model is  
 1249 incentivised to discover a small set of fundamental operations that can be recombined to solve a broad  
 1250 range of tasks, thereby fostering compositional generalisation.

1251 Formally, the loss is defined as the expected number of unique program tokens used across a  
 1252 training batch. Crucially, this expectation can be computed in a differentiable form, enabling direct  
 1253 optimisation via gradient descent.

1254 Let  $P$  denote the tensor of token probabilities output by the encoder, with dimensions  $(B, N, V)$ ,  
 1255 where  $B$  is the batch size,  $N$  is the program length, and  $V$  is the vocabulary size. The probability of  
 1256 token  $k$  being chosen at position  $i$  in sequence  $b$  is denoted  $p_{b,i,k}$ .

1257 To approximate the probability that token  $k$  never appears in the batch, we make the simplifying  
 1258 assumption that token draws are independent across positions and across examples. Under this  
 1259 assumption, the probability of never selecting token  $k$  is:

$$1261 \quad \mathbb{P}(\text{token } k \text{ never appears}) = \prod_{b=1}^B \prod_{i=1}^N (1 - p_{b,i,k}). \quad (4)$$

1264 For numerical stability, we compute this in log-space:

$$1266 \quad \log \mathbb{P}(\text{token } k \text{ never appears}) = \sum_{b=1}^B \sum_{i=1}^N \log(1 - p_{b,i,k}). \quad (5)$$

1270 The probability that token  $k$  appears at least once in the batch is therefore:

$$1272 \quad \mathbb{P}(\text{token } k \text{ appears}) = 1 - \exp \left( \sum_{b=1}^B \sum_{i=1}^N \log(1 - p_{b,i,k}) \right). \quad (6)$$

1275 By linearity of expectation, the expected number of unique tokens used in the batch is:

$$1277 \quad \mathcal{L}_{\text{reuse}} = \sum_{k=1}^V \mathbb{P}(\text{token } k \text{ appears}). \quad (7)$$

### 1280 PRACTICAL CONSIDERATIONS

1282 The token reuse loss is added to the encoder loss with weight  $\lambda_{\text{reuse}}$ . As a batch-level statistic, it can  
 1283 be sensitive to batch size and may be unstable for small batches. In practice, we used large batches  
 1284 and did not observe instabilities. Importantly, the loss must not dominate training. We therefore  
 1285 apply a very small weight, ensuring that it provides only a gentle inductive bias toward compact  
 1286 vocabularies. This prevents collapse into degenerate solutions such as a single-token language, which  
 1287 would be too limited to represent complex tasks.

1288  
 1289  
 1290  
 1291  
 1292  
 1293  
 1294  
 1295

1296 **H THE USE OF LARGE LANGUAGE MODELS (LLMs)**  
12971298 In this work, large language models (LLMs) were used solely as a tool for polishing the writing,  
1299 specifically to remove grammatical and spelling errors. They did not contribute to research ideation  
1300 or any other significant aspects of the paper.  
13011302  
1303  
1304  
1305  
1306  
1307  
1308  
1309  
1310  
1311  
1312  
1313  
1314  
1315  
1316  
1317  
1318  
1319  
1320  
1321  
1322  
1323  
1324  
1325  
1326  
1327  
1328  
1329  
1330  
1331  
1332  
1333  
1334  
1335  
1336  
1337  
1338  
1339  
1340  
1341  
1342  
1343  
1344  
1345  
1346  
1347  
1348  
1349